Available online at www.sciencedirect.com
ScienceDirect
Trans. Nonferrous Met. Soc. China 31(2021) 545−554
Transactions of Nonferrous Metals Society of China
www.tnmsc.cn

Cyclic voltammetry and potentiodynamic polarization studies of chalcopyrite concentrate in glycine medium

Maryam KHEZRI[1], Bahram REZAI[1], Ali Akbar ABDOLLAHZADEH[2], Benjamin P. WILSON[3], Mehdi MOLAEINASAB[4], Mari LUNDSTRÖM[3]

1. Department of Mining and Metallurgical Engineering, Amirkabir University of Technology (Tehran Polytechnic), Tehran, Iran;
2. Department of Mining Engineering, University of Kashan, Kashan, Iran;
3. Department of Chemical and Metallurgical Engineering (CMET), School of Chemical Engineering, Aalto University, P. O. Box 16200, Espoo, Finland;
4. Sarcheshmeh Copper Complex, National Iranian Copper Industries Company, Rafsanjan, Iran

Received 21 January 2020; accepted 30 November 2020

Abstract: Cyclic voltammetry and potentiodynamic polarization analyses were utilized to investigate the mechanism and kinetics of glycine leaching reactions for chalcopyrite. The effects of pH (9−12), temperature (30−90 °C) and glycine concentration (0−2 mol/L) on corrosion current density, corrosion potential and cyclic voltammograms were investigated using chalcopyrite concentrate−carbon paste electrodes. Results showed that an increase in the glycine concentration from 0 to 2 mol/L led to an increased oxidation peak current density. Under the same conditions, corrosion current density was found to change from approximately 28 to 89 μA/cm^2, whereas corrosion potential was decreased from −80 to −130 mV. Elevated temperatures enhanced the measured current densities up to 60 °C; however, above this level, current density was observed to decrease. A similar current density behavior was determined with pH. A pH change from 9 to 10.5 resulted in an increase in current density and pH higher than 10.5 gave rise to a reduced current density. In addition, the thermodynamic stability of copper and iron oxides was found to increase at higher temperatures.

Key words: glycine; corrosion current density; corrosion potential; electrochemical behaior; chalcopyrite concentrate

1 Introduction

The development of more environmentally sustainable alternative hydrometallurgical leaching routes that allow more efficient processing of sulfide minerals like chalcopyrite, the most abundant and resistant copper-bearing mineral, are of significant importance [1,2]. For example, glycine ($H_2N—CH_2—COOH$) leaching of chalcopyrite ores and concentrates under alkaline conditions has been the subject of increasing interest in the last few years [3−8]. Glycine acts as a complexing reagent that leads to the formation of a copper glycinate complex ($Cu(NH_2CH_2COO)_2$) during the process and in general, the dissolution mechanism of metallic sulfides in aqueous solutions involves electrochemical reaction pathways [9].

Electrochemical analyses have been performed to study the anodic dissolution of chalcopyrite in sulphate, nitrate, and chloride media [10−16] and a small pre-wave attributed to the surface oxidation of chalcopyrite has been observed in some of these studies [10,16,17]. Electrochemical investigations on cathodic polarization, constant potential and cyclic polarization of $CuFeS_2$ minerals in H_2SO_4-based electrolytes have indicated that thin, generally porous layers of copper−iron sulfides

Corresponding author: Bahram REZAI, Tel: +98-21-64542953; Fax: +98-21-66405846; E-mail: pro.bahram.rezai@gmail.com
DOI: 10.1016/S1003-6326(21)65516-4

initially form and these may even include chalcocite or djurleite ($Cu_{1.9}S$) products [18]. Additionally, electrochemical investigations using an electrode formed from massive chalcopyrite have shown that during chalcopyrite dissolution, a passive layer composed of sulfides, polysulfides and elemental sulfur is formed on the mineral surface [19]. Further studies of this phenomenon have suggested that a metal deficient polysulfide semi-conductor film is formed on the surface of chalcopyrite during leaching and this leads to a reduction in the transfer rate of both ions and electrons [20]. Similar research of chalcopyrite in alkaline glycine solutions by a chalcopyrite rotating disk electrode has shown that iron oxyhydroxides, elemental sulfur and porous disulfide layers are formed on the mineral surface. But these surface layers had no passivating behavior [5]. Nevertheless, although there are numerous publications [5,10,19,21−24] related to the anodic dissolution of chalcopyrite in a different media, electrochemical analyses by cyclic voltammetry and potentiodynamic polarization methods in alkaline glycine solution at high temperature and high glycine concentration have not yet been well investigated. Consequently, in this research the mechanism and kinetics of chalcopyrite dissolution and the effect of several key parameters including temperature, pH and glycine concentration were investigated by cyclic voltammetry and potentiodynamic polarization methods in a three-electrode cell to provide a more detailed insight of the reactions.

2 Experimental

2.1 Materials

A chalcopyrite concentrate flotation sample was obtained from Sarcheshmeh Copper Mine (Kerman, Iran). It was dried and analyzed by X-ray diffractometry (XRD), X-ray fluorescence (XRF) and atomic absorbance spectrophotometry (AAS). Results of XRD analysis showed that the main phases of the concentrate were chalcopyrite (70%) and pyrite (9%), whereas the associated chemical compositions of the concentrate determined with XRF and AAS are displayed in Table 1. All experimental solutions were prepared from analytical grade reagents and deionized water. The chalcopyrite concentrate with a d_{80} of 75 μm at a slurry density of 50% (400 g concentrate for each batch) and Calgon addition of 1% (as grinding aid) were ground in a ball mill for 5 h with a rotation speed of 70 r/min and 3660 g steel balls (ball diameter is 6.5−15 mm). The resulting pulp was then filtered and dried in an oven at 75 °C for 12 h.

Table 1 Chemical compositions of chalcopyrite concentrate based on XRF and AAS (for Cu) (wt.%)

Fe	Cu	CuO	S	SiO_2	Al_2O_3	Mo
26.8	24.2	0.9	30.5	4.8	1.6	0.1

2.2 Methods

Electrochemical analyses (cyclic voltammetry and potentiodynamic polarization) were carried out with a conventional three-electrode cell set-up with thermostatic control (Fig. 1), using an Autolab potentiostat (Ecochemie, Netherlands) with GPES software. The electrodes used included a chalcopyrite concentrate−carbon paste working electrode (WE), a perforated platinum plate counter electrode (CE) and a Ag/AgCl (3 mol/L KCl) reference electrode (RE), which was held in a Luggin-Haber capillary that contained a 0.5 mol/L KCl solution. In order to prepare the carbon paste electrode, graphite powder (0.7 g, ~38 μm, Merck, Germany), the re-ground chalcopyrite concentrate (0.3 g, d_{80}=11 μm which was measured with a laser particle size analyzer (Malvern Mastersizer 3000, Malvern, UK)) and 5 drops of paraffin oil (Merck, Germany) were completely mixed. Once completely homogenized, the paste was placed on a carbon layer within a small hole (surface area of 0.44 cm^2) on the top of a copper plate mounted in epoxy. Electrolytes with different concentrations of glycine were prepared with deionized water and the desired pH of the solutions was achieved by adjustment with 1 mol/L NaOH. Temperature control of the electrochemical cell was provided by a thermostatic circulating water bath and all electrolyte solutions were purged with nitrogen for 15 min prior to measurement in order to eliminate any effect of oxygen. Electrochemical measurements were performed by sweeping the potential in the positive direction from −500 to 500 mV at a scan rate of 20 mV/s. In addition, Pourbaix diagrams (φ−pH diagrams) for the Cu−Fe−S−glycine system at different glycine concentrations (0−2 mol/L) and temperatures (30−90 °C) were obtained using HSC Chemistry

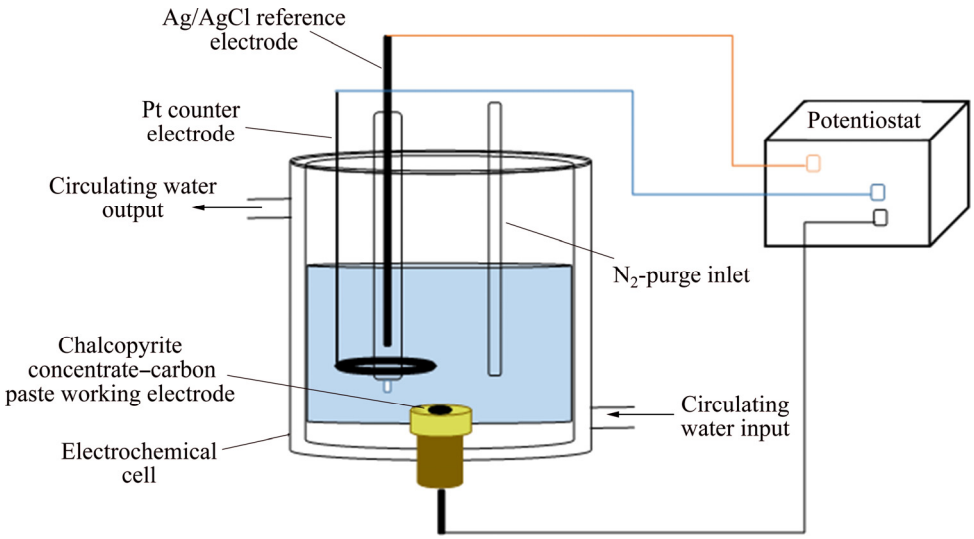

Fig. 1 Schematic diagram of three-electrode electrochemical cell used

software (HSC Chemistry Version 6, Outotec Oy, Finland) to more fully understand the reactions occurring during the leaching process.

Corrosion current densities and corrosion potentials were obtained from the intersections of tangent lines of cathodic and anodic branches in Tafel plots.

3 Results and discussion

In order to gain a better understanding of the dissolution behavior of chalcopyrite concentrate in glycine medium, electrochemical studies (cyclic voltammetry and potentiodynamic polarization) were performed at different pH (9, 10.5 and 12), temperatures (30−90 °C) and glycine concentrations (0−2 mol/L) to determine their effects on the anodic and cathodic behavior of a chalcopyrite concentrate−carbon paste electrode.

3.1 Effect of glycine concentration

The effect of glycine concentration on the copper dissolution from chalcopyrite concentrate was investigated by carrying out cyclic voltammetry and potentiodynamic polarization studies in solutions with glycine concentrations between 0 and 2 mol/L. Cyclic voltammograms for the chalcopyrite concentrate−carbon paste working electrode in different glycine electrolyte solutions at 60 °C and initial solution pH 10.5 are shown in Fig. 2. As can be seen, at all glycine concentrations investigated, no marked increase in the level of current density is observed up to −100 mV; however, when the potential increases to 20 mV it is clear that higher glycine concentrations result in enhanced current density levels (Fig. 2). Pourbaix diagrams for the Cu−Fe−S−glycine system at different glycine concentrations are displayed in Fig. 3. As can be seen, an increased glycine concentration enhances the copper glycinate stability region, which gives rise to the increased current densities as reported previously [5]. In the first scan, an anodic reaction (Eq. (1)) is supposed to be related to the oxidation of chalcopyrite as the main phase in the sample.

$$CuFeS_2+2HGly+21OH^-=Cu(Gly)_2+0.5Fe_2O_3+2SO_4^{2-}+11.5H_2O+17e \quad (1)$$

At low concentration of glycine (0.4 mol/L), an increase in the applied potential from the open circuit potential (OCP) of −130 mV results in a gradual increase in current density, which indicates that a low level of copper dissolution can occur at such a concentration.

It was reported that in the presence of Cu^+, chalcopyrite is reduced to burnite and then to chalcocite at potentials around 0 mV according to Eqs. (2) and (3), respectively [25]:

$$2CuFeS_2+3Cu^++e=Cu_5FeS_4+Fe^{2+} \quad (2)$$

$$Cu_5FeS_4+3Cu^++e=4Cu_2S+Fe^{2+} \quad (3)$$

Chalcocite is also formed according to the following equation in alkaline media [26]:

$$2Cu^{2+}+HS^-+OH^-=Cu_2S+H_2O+2e \quad (4)$$

The existence of an anodic peak in potential range from −100 to 20 mV, in the second and third

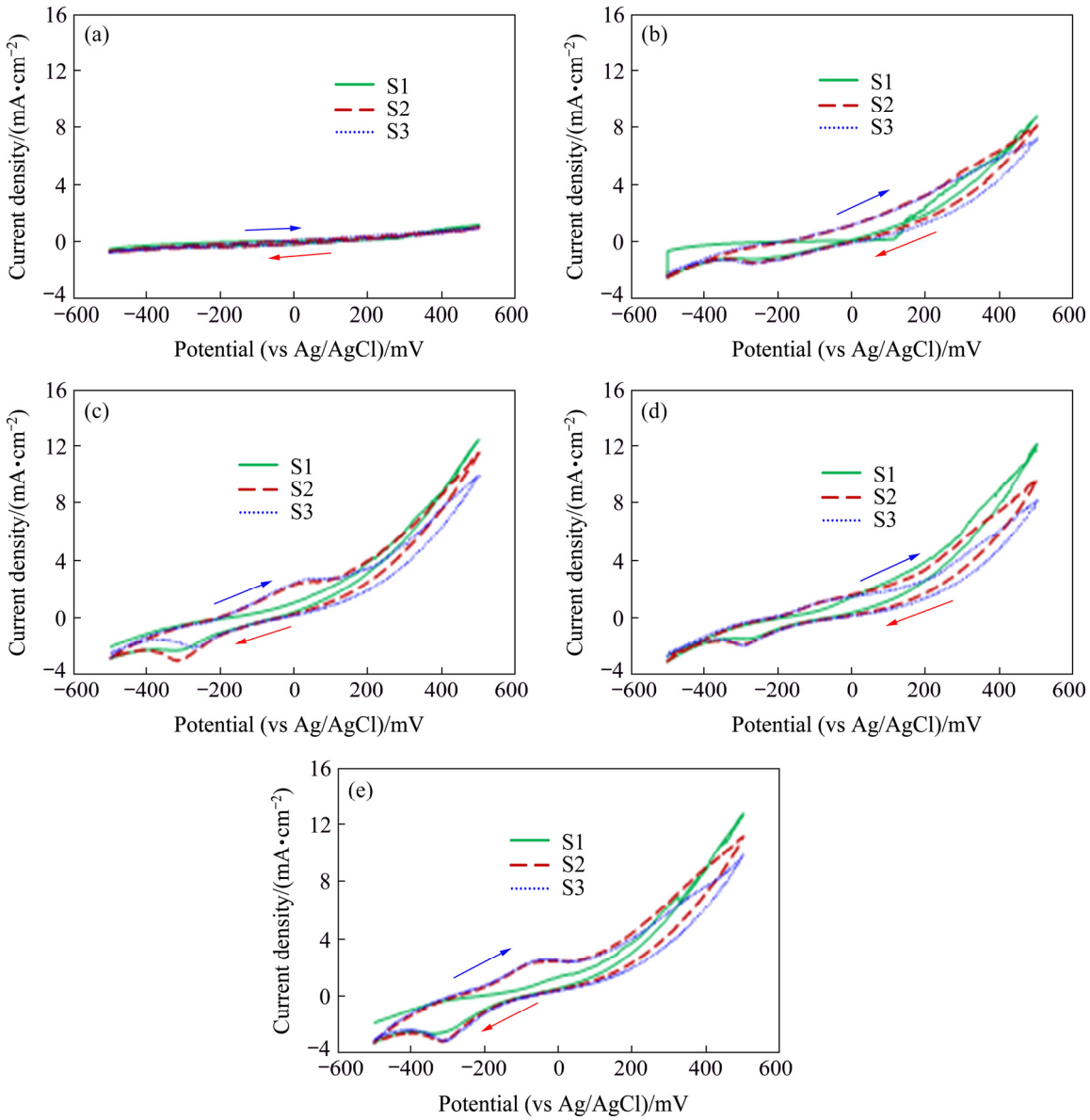

Fig. 2 Cyclic voltammograms of conventional ball-milled chalcopyrite concentrate−carbon paste electrodes at different glycine concentrations: (a) 0 mol/L; (b) 0.4 mol/L; (c) 0.7 mol/L; (d) 1 mol/L; (e) 2 mol/L (Initial solution pH 10.5, 60 °C and atmospheric pressure; S1: First scan, S2: Second scan, and S3: Third scan)

scans can be due to the oxidation of chalcocite (Eq. (5)) which could be formed during the previous cathodic scan according to Eqs. (2) and (3) and chemical precipitation of chalcocite (Eq. (4)).

Chalcocite is then oxidized to covellite (CuS) and copper glycinate in the anodic oxidation of the next scans according to Eq. (5):

$$Cu_2S+2NH_2CH_2COOH+0.5O_2= Cu(NH_2CH_2COO)_2+CuS+H_2O \quad (5)$$

It has been reported that covellite is slowly leached in the glycine medium according to Eq. (6) [27]:

$$CuS+2NH_2CH_2COOH+2O_2+2OH^-= Cu(NH_2CH_2COO)_2+SO_4^{2-}+2H_2O \quad (6)$$

This oxidation reaction can be a rate-limiting step during the overall dissolution of copper from chalcopyrite.

As can be seen from the Pourbaix diagrams (Fig. 3), in the potential range from −300 to 0 mV (vs Ag/AgCl) at pH ~10.5, Cu-oxyhydroxide and copper sulfide (Cu, $Cu(OH)_2$, Cu_2O, Cu_2S) and Fe-oxide (Fe_2O_3, Fe_3O_4) solid phases are thermodynamically stable. This finding correlates with the presence of iron oxyhydroxides and copper

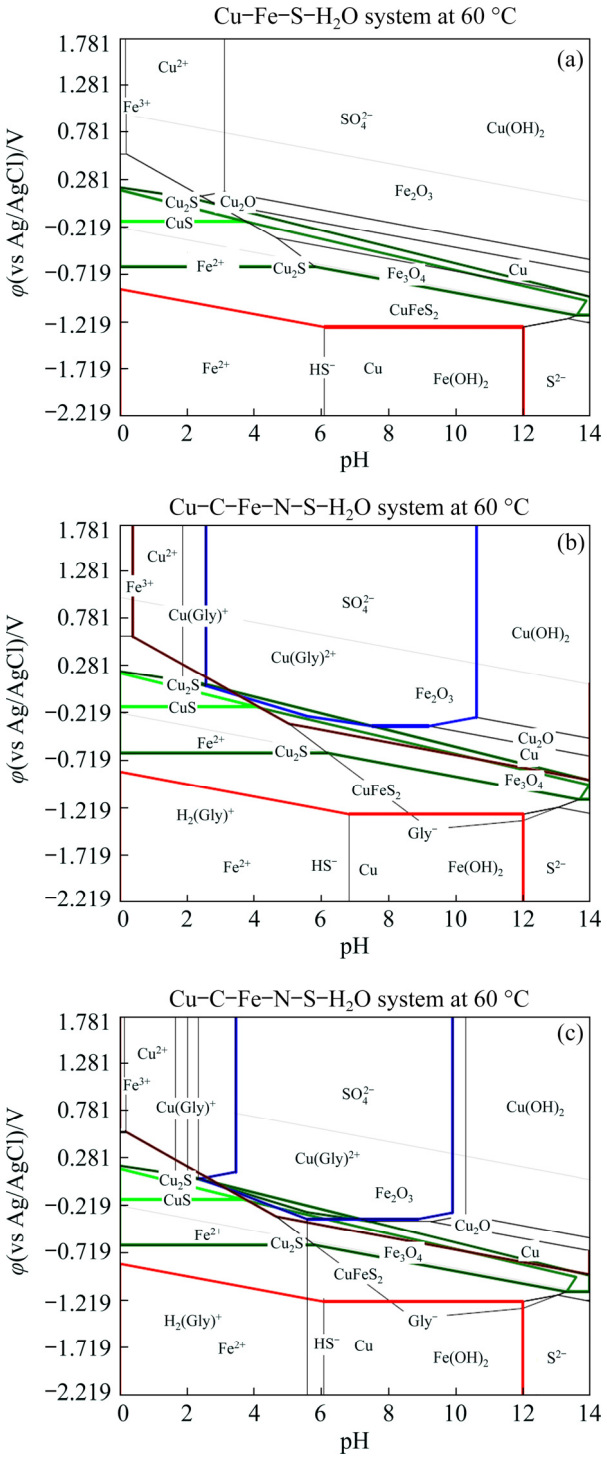

Fig. 3 φ–pH diagrams for Cu−Fe−S−glycine at 60 °C and different glycine concentrations: (a) 0 mol/L; (b) 0.7 mol/L; (c) 2 mol/L

oxides, copper sulfide and copper sulfate layers detailed in previous studies [5,7,8]. In our recent research [28] covellite (CuS) and maghemite (γ-Fe_2O_3) have been found in the leach residue. Recently, the formation of iron oxide passive layers on the surface of chalcopyrite has been found to occur in an ammonia–ammonium chloride system [29].

The relatively flat shape of the current density−potential curves in Fig. 2(a) highlights that the chalcopyrite is unable to dissolve when glycine is absent from solution.

Figure 4 displays the polarization curves for the chalcopyrite concentrate−carbon paste working electrode at different glycine concentrations and the data obtained from these curves are listed in Table 2. As glycine concentration increases from 0 to 2 mol/L, there is a clear enhancement of the corrosion current density (J_{corr}), which increases from 28.2 to 89.1 μA/cm^2, whilst there is a decrease in the corrosion potential (φ_{corr}).

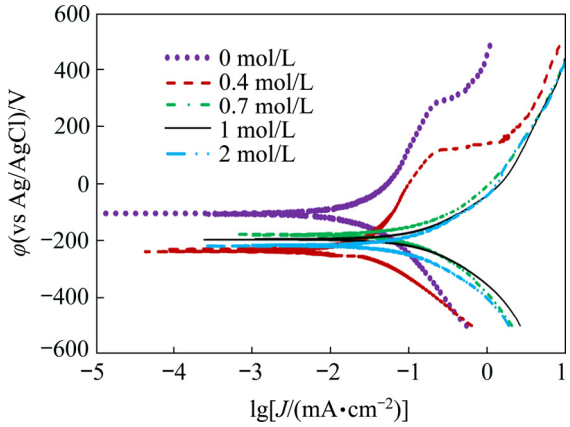

Fig. 4 Polarization curves of conventional ball-milled chalcopyrite concentrate−carbon paste electrodes at different glycine concentrations (Initial solution pH 10.5, 60 °C and atmospheric pressure)

Table 2 Data from polarization curves of conventional ball-milled chalcopyrite concentrate−carbon paste electrodes at different glycine concentrations (Initial solution pH 10.5, 60 °C and atmospheric pressure)

Glycine concentration/(mol·L^{-1})	φ^*_{corr} (vs Ag/AgCl)/mV	J_{corr}/(μA·cm^{-2})
0	−100	28.2
0.4	−230	35.5
0.7	−180	79.4
1	−200	89.1
2	−220	89.1

* Corrosion potential was measured in 3 mol/L KCl solution

3.2 Effect of pH

In order to investigate the effect of pH on the copper dissolution from the chalcopyrite

concentrate, cyclic voltammetry and potentiodynamic polarization studies were performed using the chalcopyrite concentrate−carbon paste working electrode with a glycine concentration of 0.7 mol/L, temperature of 60 °C and different initial pH ranging from 9 to 12 (Fig. 5). The effect of pH on the cyclic voltammograms is clearly shown, as shown in Fig. 5(a), the shape of the current density−potential curve at pH 9 is relatively flat, which indicates that no dissolution takes place as a result of a decrease in mole fraction of glycinate anion [30]. In comparison, the curves measured at pH>9, presented in Figs. 5(b) and (c), show an increase in current density at potentials above −100 mV. The maximum current density is observed at pH 10.5 (Fig. 5(b)), which indicates that the maximum level extraction of copper takes place and there is a clear anodic current peak in the second and third scans at around 40 mV that relates to the anodic dissolution of electroactive specimens (Cu_2S and CuS) in the glycine medium (Eqs. (5) and (6)). In contrast, Fig. 5(c) shows that when pH 12 is used, the current density only increases gradually with higher levels of applied potentials, which clearly demonstrates that the rate of copper dissolution is lower that at pH 10.5 and this probably results from the higher stability of copper oxides like CuO and Cu_2O compared to copper glycinate [5]. Moreover, it is clear from the subsequent scans at pH 12 that the current density continues to decrease, from which it can be concluded that this pH is more thermodynamically favourable to form species such as Cu oxides and this results in the lower current densities.

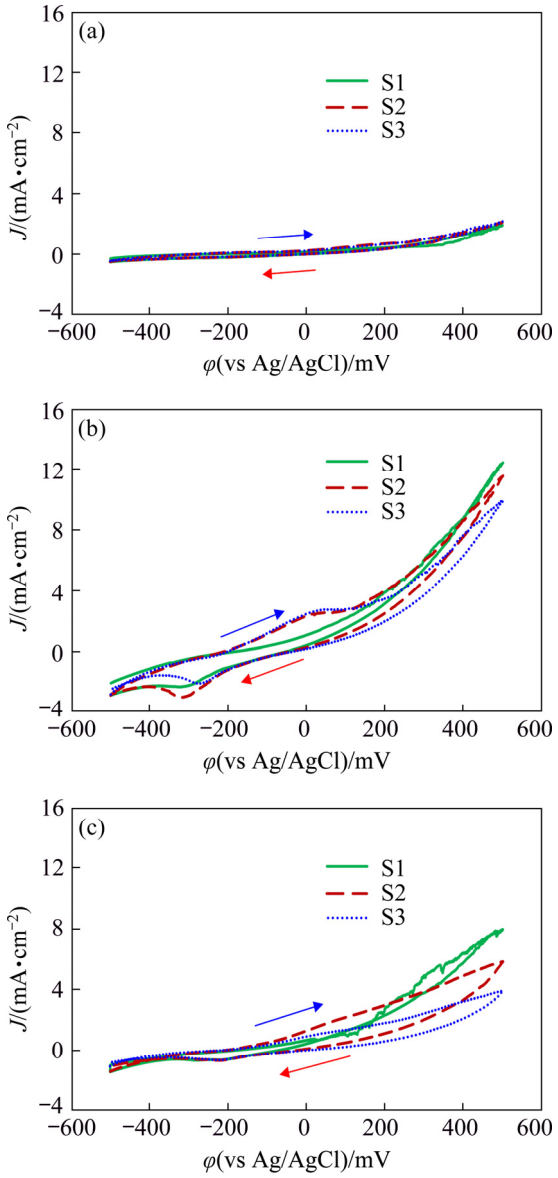

Fig. 5 Cyclic voltammograms of conventional ball-milled chalcopyrite concentrate−carbon paste electrodes at glycine concentration of 0.7 mol/L, 60 °C, atomspheric pressure, and different initial solution pH levels: (a) pH 9; (b) pH 10.5; (c) pH 12

Polarization curves measured with the chalcopyrite concentrate−carbon paste electrode at different pH levels are shown in Fig. 6 and the data obtained from these curves are displayed in Table 3. As can be seen, when pH increases there is only a small difference in the corrosion potentials recorded. On the other hand, the behavior of the corrosion current density displays a more active behavior, for example, when the pH increases from 9 to 10.5 the corrosion current density is increased by over 5 times from 12.6 to a maximum of 79.4 μA/cm^2. Above pH 10.5, the corrosion current density is reduced, which once again indicates the presence of a surface layer.

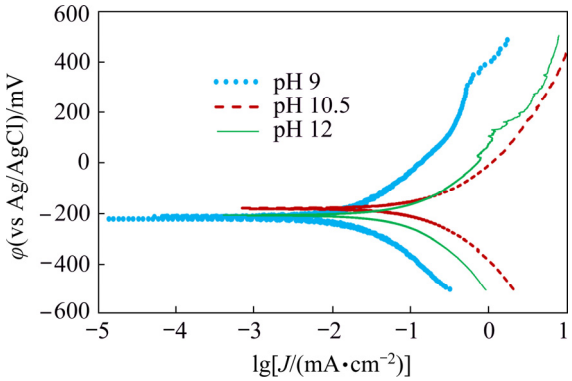

Fig. 6 Polarization curves of conventional ball-milled chalcopyrite concentrate−carbon paste electrodes at glycine concentration of 0.7 mol/L, 60 °C, atmospheric pressure and different initial solution pH levels

Table 3 Data from polarization curves of conventional ball-milled chalcopyrite concentrate−carbon paste electrodes at different initial pH levels (Glycine concentration of 0.7 mol/L, 60 °C and atmospheric pressure)

pH	φ^*_{corr} (vs Ag/AgCl)/mV	J_{corr}/(μA·cm^{-2})
9	−220	12.6
10.5	−180	79.4
12	−205	56.2

* Corrosion potential was measured in 3 mol/L KCl solution

3.3 Effect of temperature

As temperature is one of the most important parameters that affect the dissolution rate of copper from chalcopyrite concentrate, electrochemical studies were performed with the chalcopyrite concentrate−carbon paste working electrode at a glycine concentration of 0.7 mol/L, initial pH of 10.5 and over a temperature range from 30 to 90 °C (Fig. 7). As can be seen from Fig. 7(a), the cyclic voltammogram at 30 °C is relatively flat as no obvious dissolution takes place. At 60 and 90 °C (Figs. 7(b) and (c)), when the applied potentials are higher than −100 mV, an increase in current density can be observed and a clear anodic current density peak between −100 and 20 mV related to electroactive specimen dissolution (Eqs. (5) and (6)) is evident. Nevertheless, the current density of this anodic peak is found to decrease from about 2.5 to about 1.8 mA/cm^2 as temperature increases from 60 to 90 °C and the current density continues to decrease in the subsequent scans at 90 °C. The analysis of the related Pourbaix diagrams for the Cu−Fe−S−glycine system at different temperatures displayed in Fig. 8 shows that at pH 10.5, in an applied potential range from −300 to 0 mV (vs Ag/AgCl), copper is initially dissolved as copper glycinate complex. This dissolved copper in the presence of Fe-ions can subsequently be changed into Cu-oxyhydroxides, copper sulfide (Cu, $Cu(OH)_2$, Cu_2O, Cu_2S) and Fe-oxides (Fe_2O_3, Fe_3O_4). As temperature increases (Figs. 8(b) and (c)), the stability region of the copper glycinate is shown to decrease, whereas the stability regions for Cu, $Cu(OH)_2$, Cu_2O, Fe_3O_4 and Fe_2O_3 solid phases all become enlarged. In other words, an increase in temperature leads to a concurrent decrease in the rate of copper dissolution and an increase in the thermodynamic stability of the secondary phase formation. Previous studies reported that iron hydroxide oxides, copper oxides (like CuO, Cu_2O) and sulfides/sulfates can be formed during the chalcopyrite leaching in glycine medium [5,7,8] and O′CONNOR et al [30] have shown that at higher temperatures, the stability region for copper glycinate is reduced.

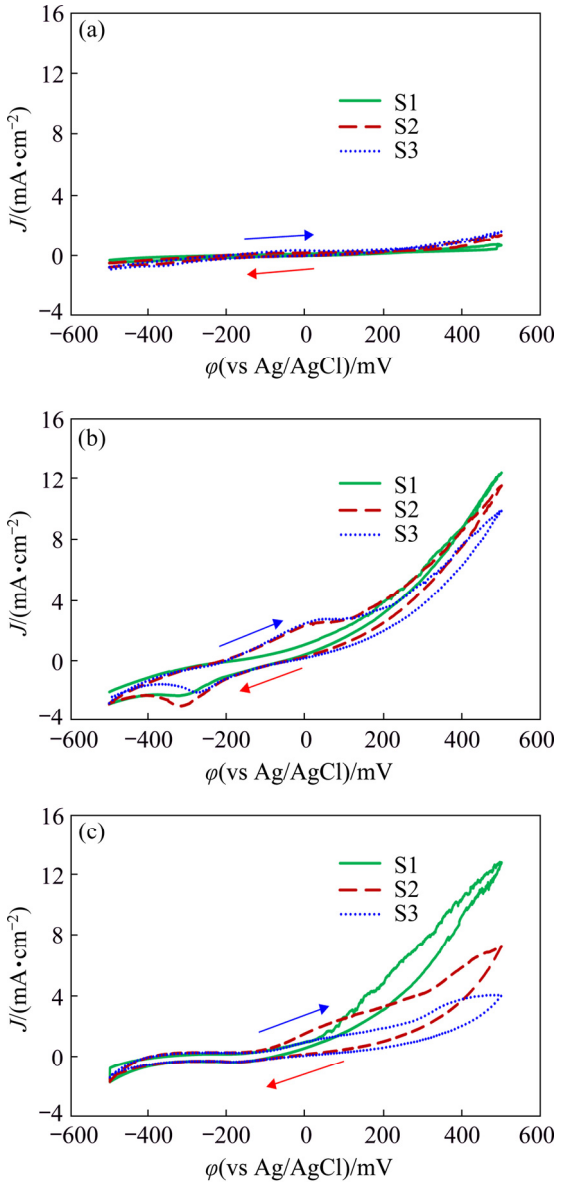

Fig. 7 Cyclic voltammograms of conventional ball-milled chalcopyrite concentrate−carbon paste electrodes at glycine concentration of 0.7 mol/L, initial pH of 10.5, atmospheric pressure and different temperatures: (a) 30 °C; (b) 60 °C; (c) 90 °C

Polarization curves of chalcopyrite concentrate−carbon electrode at different temperatures are shown in Fig. 9 and the associated electrochemical data obtained are displayed in Table 4. When the

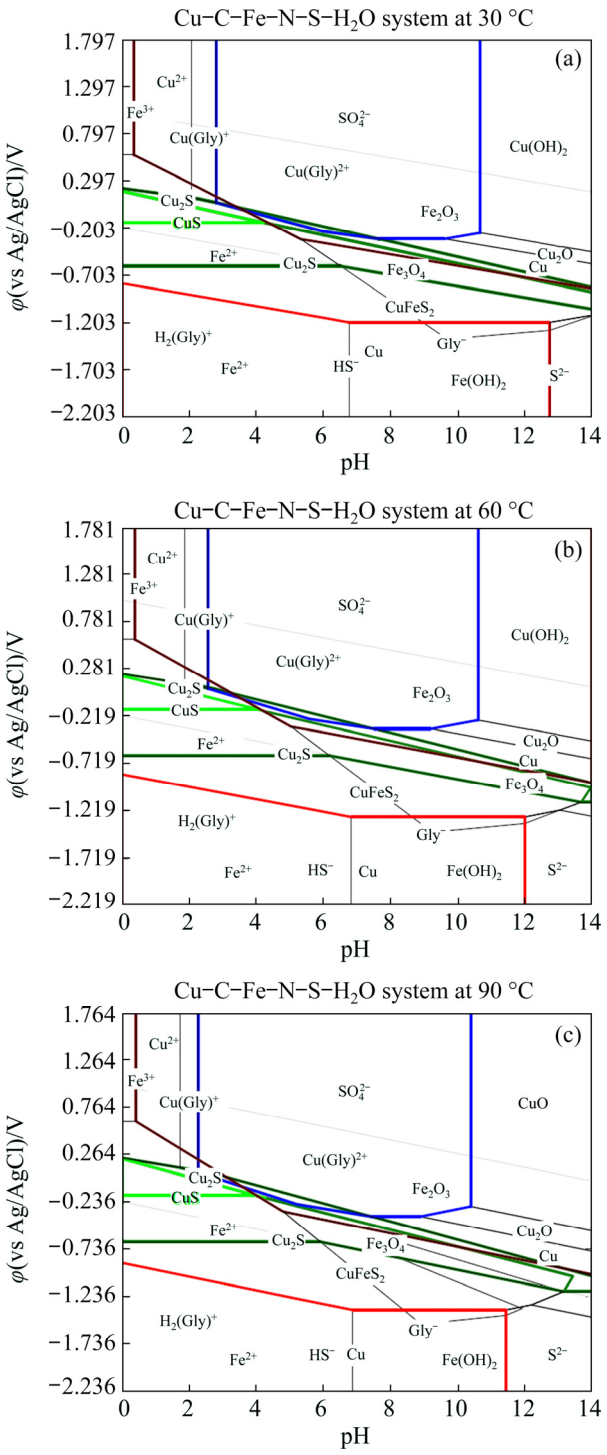

Fig. 8 φ−pH diagrams for Cu−Fe−S−glycine system at different temperatures: (a) 30 °C; (b) 60 °C; (c) 90 °C

temperature is raised to 60 °C, the rate of copper dissolution increases and this rate is greater than the rate of copper removal, which leads to the maximum corrosion current density of the system. As the temperature is further increased, the rate of copper removal starts to become close to the rate of copper dissolution, leading to the measured decrease in corrosion current density in Fig. 9 and this observation correlates with the thermodynamic interpretations outlined here.

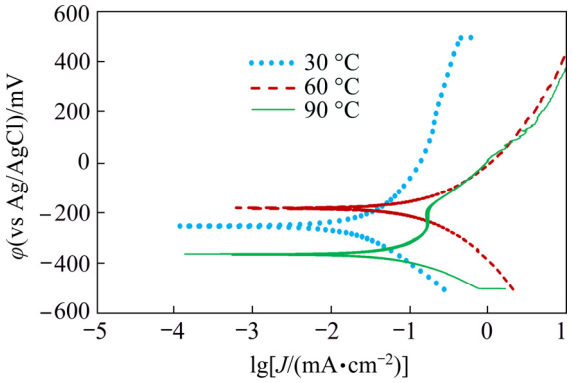

Fig. 9 Polarization curves of conventional ball-milled chalcopyrite concentrate−carbon paste electrodes at glycine concentration of 0.7 mol/L, initial pH of 10.5, atmospheric pressure and different temperatures

Table 4 Data from polarization curves of conventional ball-milled chalcopyrite concentrate−carbon paste electrodes at different temperatures (Glycine concentration of 0.7 mol/L, initial pH of 10.5 and atmospheric pressure)

Temperature/ °C	φ^*_{corr} (vs Ag/AgCl)/ mV	J_{corr}/ (μA·cm^{-2})
30	−250	25.1
60	−180	79.4
90	−360	56.2

* Corrosion potential was measured in 3 mol/L KCl solution

4 Conclusions

(1) In the applied potential range from −100 to 20 mV, an increase in glycine concentration results in an increase in anodic current density as a consequence of enhanced glycinate ion concentrations. This was confirmed by φ−pH diagrams, which showed that an increase in glycine concentration led to an enhanced copper glycinate stability.

(2) In the absence of glycine, with increasing applied potential, the anodic current density is not increased (a flat shape), which indicates no dissolution of the mineral in the potential range.

(3) With increasing temperature up to 60 °C, current density is increased. Higher temperature leads to a decrease in current density, probably due to smaller stability region of copper glycinate and wider stability region for Cu-oxyhydroxides and

iron oxides at higher temperatures.

(4) The current density is increased up to the pH of 10.5, while it is decreased at the pH of 12 probably due to lower stability of copper glycinate and higher thermodynamic stability of secondary phases of copper oxyhydroxides, copper sulfides and iron oxides.

Acknowledgments

This study was funded by National Copper Industries Company (Iran). In addition, the authors would like to acknowledge the Hydrometallurgy and Corrosion Group in the Department of Chemical and Metallurgical Engineering at the School of Chemical Engineering, Aalto University (Finland) for providing equipment and materials.

References

[1] LUNDSTRÖM M. Chalcopyrite dissolution in cupric chloride solutions [D]. Espoo: Aalto University, 2009.

[2] PRICE D, WARREN G. The influence of silver ion on the electrochemical response of chalcopyrite and other mineral sulfide electrodes in sulfuric acid [J]. Hydrometallurgy, 1986, 15: 303−324.

[3] EKSTEEN J, ORABY E, TANDA B. A conceptual process for copper extraction from chalcopyrite in alkaline glycinate solutions [J]. Minerals Engineering, 2017, 108: 53−66.

[4] TANDA B, ORABY E, EKSTEEN J. Recovery of copper from alkaline glycine leach solution using solvent extraction [J]. Separation and Purification Technology, 2017, 187: 389−396.

[5] O'CONNOR G, LEPKOVA K, EKSTEEN J, ORABY E. Electrochemical behaviour and surface analysis of chalcopyrite in alkaline glycine solutions [J]. Hydrometallurgy, 2018, 182: 32−43.

[6] EKSTEEN J, ORABY E, TANDA B. An alkaline glycine-based process for copper recovery and iron rejection from chalcopyrite [C]//Proceedings of the IMPC. Perth, 2016: 158−167.

[7] SHIN D, AHN J, LEE J. Kinetic study of copper leaching from chalcopyrite concentrate in alkaline glycine solution [J]. Hydrometallurgy, 2019, 183: 71−78.

[8] TANDA B, EKSTEEN J, ORABY E, O'CONNOR G. The kinetics of chalcopyrite leaching in alkaline glycine/glycinate solutions [J]. Minerals Engineering, 2019, 135: 118−128.

[9] HABASHI F. Dissolution of minerals and hydrometallurgical processes [J]. The Science of Nature, 1983, 70: 403−411.

[10] BIEGLER T, SWIFT D. Anodic electrochemistry of chalcopyrite [J]. Journal of Applied Electrochemistry, 1979, 9: 545−554.

[11] MAJUSTE B, CIMINELLI V, OSSEO-ASARE K, DANTAS M, MAGALHÃES-PANIAGO R. Electrochemical dissolution of chalcopyrite: Detection of bornite by synchrotron small angle X-ray diffraction and its correlation with the hindered dissolution process [J]. Hydrometallurgy, 2012, 111: 114−123.

[12] LÁZARO I, MARTÍNEZ-MEDINA N, RODRÍGUEZ I, ARCE E, GONZÁLEZ I. The use of carbon paste electrodes with non-conducting binder for the study of minerals: Chalcopyrite [J]. Hydrometallurgy, 1995, 38: 277−287.

[13] SAUBER M, DIXON D G. Electrochemical study of leached chalcopyrite using solid paraffin-based carbon paste electrodes [J]. Hydrometallurgy, 2011, 110: 1−12.

[14] DAS CHAGAS ALMEIDA T, GARCIA E M, DA SILVA H, MATENCIO T, LINS V. Electrochemical study of chalcopyrite dissolution in sulfuric, nitric and hydrochloric acid solutions [J]. International Journal of Mineral Processing, 2016, 149: 25−33.

[15] LU Z, JEFFREY M, LAWSON F. An electrochemical study of the effect of chloride ions on the dissolution of chalcopyrite in acidic solutions [J]. Hydrometallurgy, 2000, 56: 145−155.

[16] BIEGLER T, HORNE M. The electrochemistry of surface oxidation of chalcopyrite [J]. Journal of the Electrochemical Society, 1985, 132: 1363−1369.

[17] JUAN Y U, YANG H Y, FAN Y J. Effect of potential on characteristics of surface film on natural chalcopyrite [J]. Transactions of Nonferrous Metals Society of China, 2011, 21(8): 1880−1886.

[18] WARREN G, SOHN H J, WADSWORTH M, WANG T. The effect of electrolyte composition on the cathodic reduction of $CuFeS_2$ [J]. Hydrometallurgy, 1985, 14: 133−149.

[19] GOMEZ C, FIGUEROA M, MUNOZ J, BLÁZQUEZ M, BALLESTER A. Electrochemistry of chalcopyrite [J]. Hydrometallurgy, 1996, 43: 331−344.

[20] PARKER A, PAUL R, POWER G. Electrochemistry of the oxidative leaching of copper from chalcopyrite [J]. Journal of Electroanalytical Chemistry and Interfacial Electrochemistry, 1981, 118: 305−316.

[21] HIROYOSHI N, KUROIWA S, MIKI H, TSUNEKAWA M, HIRAJIMA T. Synergistic effect of cupric and ferrous ions on active-passive behavior in anodic dissolution of chalcopyrite in sulfuric acid solutions [J]. Hydrometallurgy, 2004, 74: 103−116.

[22] DUTRIZAC J. The dissolution of chalcopyrite in ferric sulfate and ferric chloride media [J]. Metallurgical Transactions B, 1981, 12: 371−378.

[23] MCMILLAN R, MACKINNON D, DUTRIZAC J. Anodic dissolution of n-type and p-type chalcopyrite [J]. Journal of Applied Electrochemistry, 1982, 12: 743−757.

[24] LAZARO I, NICOL M. A rotating ring–disk study of the initial stages of the anodic dissolution of chalcopyrite in acidic solutions [J]. Journal of Applied Electrochemistry, 2006, 36: 425−431.

[25] MACLEOD I D, MUIR D M. Reduction of chalcopyrite with copper (I) [J]. Journal of Applied Electrochemistry, 1983, 13: 411−416.

[26] FERNÁNDEZ-REYES J S, GARCÍA-MEZA J V. Bioelectrochemical system for the biooxidation of a chalcopyrite concentrate by acidophilic bacteria coupled to energy current generation and cathodic copper recovery [J]. Biotechnology Letters, 2018, 40: 63−73.

[27] TANDA B, EKSTEEN J, ORABY E. Kinetics of chalcocite leaching in oxygenated alkaline glycine solutions [J]. Hydrometallurgy, 2018, 178: 264−273.
[28] KHEZRI M, REZAI B, ABDOLLAHZADEH A A, WILSON B P, MOLAEINASAB M, LUNDSTRÖM M. Investigation into the effect of mechanical activation on the leaching of chalcopyrite in a glycine medium [J]. Hydrometallurgy, 2020: 105492.
[29] HUA X M, ZHENG Y F, QIAN X U, LU X G, CHENG H W, ZOU X L, SONG Q S, NING Z Q. Interfacial reactions of chalcopyrite in ammonia–ammonium chloride solution [J]. Transactions of Nonferrous Metals Society of China, 2018, 28(3): 556−566.
[30] O′CONNOR G, LEPKOVA K, EKSTEEN J, ORABY E. Electrochemical behaviour of copper in alkaline glycine solutions [J]. Hydrometallurgy, 2018, 181: 221−229.

黄铜矿精矿在甘氨酸介质中的循环伏安及动电位极化研究

Maryam KHEZRI[1], Bahram REZAI[1], Ali Akbar ABDOLLAHZADEH[2], Benjamin P. WILSON[3], Mehdi MOLAEINASAB[4], Mari LUNDSTRÖM[3]

1. Department of Mining and Metallurgical Engineering, Amirkabir University of Technology (Tehran Polytechnic), Tehran, Iran;
2. Department of Mining Engineering, University of Kashan, Kashan, Iran;
3. Department of Chemical and Metallurgical Engineering (CMET), School of Chemical Engineering, Aalto University, P. O. Box 16200, Espoo, Finland;
4. Sarcheshmeh Copper Complex, National Iranian Copper Industries Company, Rafsanjan, Iran

摘　要：采用循环伏安及动电位极化方法研究黄铜矿在甘氨酸介质中的浸出反应机理及动力学。使用黄铜精矿−碳糊电极研究 pH 值 (9~12)，温度 (30~90 °C)及甘氨酸浓度 (0~2 mol/L)对腐蚀电流密度、腐蚀电位及循环伏安曲线的影响。结果显示，甘氨酸浓度从 0 增加到 2 mol/L 导致氧化峰电流密度增加；在相同条件下，腐蚀电流密度从约 28 μA/cm^2 增加至约 89 μA/cm^2，同时腐蚀电位由−80 mV 降至−130 mV。在温度不高于 60 °C 的条件下，电流密度随温度的增加而增加；当温度高于 60 °C 时，电流密度随温度增加而降低。电流密度随 pH 值的变化与温度相似，当 pH 值从 9 增至 10.5 时电流密度增加，pH 值高于 10.5 时电流密度降低。此外，铜氧化物及铁氧化物的热力学稳定性在较高温度下增加。

关键词：甘氨酸；腐蚀电流密度；腐蚀电位；电化学行为；黄铜矿精矿

(Edited by Wei-ping CHEN)